Method for determining photoelectron angular distribution, total cross section and excitation beam polarisation from measurement of the integrated flux into selected solid angles

1983 J. Phys. B: At. Mol. Phys. 16 4467

(http://iopscience.iop.org/0022-3700/16/23/027)

J. Phys. B: At. Mol. Phys. **16** (1983) 4467–4480. Printed in Great Britain

Method for determining photoelectron angular distribution, total cross section and excitation beam polarisation from measurement of the integrated flux into selected solid angles

W D Grobman†, R Willoughby† and R N Zare‡

† IBM T J Watson Research Center, Yorktown Heights, New York 10598, USA
‡ Department of Chemistry, Stanford University, Stanford, California 94305, USA

Received 11 May 1983

Abstract. Detector geometries may be chosen to determine the total cross section σ_{tot}, the asymmetry parameter β and the photon polarisation p while achieving good experimental statistics by using large acceptance angles in gas-phase photoemission experiments, in which the emitted electron current distribution is described by $\sigma_{tot}[1+\beta P_2(\cos\gamma)]/4\pi$, where γ is the angle between the emitted electron and the direction of one of the polarisation components of the photon beam. When a cylindrical mirror analyser (CMA) with variable acceptance geometry is used, it is possible to determine σ_{tot}, β and the incident light polarisation p by measuring the flux with several different restricted (vignetted) annular rings whose polar and azimuthal angular acceptance ranges are appropriately chosen. The mathematical structure of this problem precludes determination of σ_{tot}, β and p from the measured photocurrent using a CMA having its aperture vignetted only in the azimuthal or polar angle. However, these three parameters can be found when the aperture is independently vignetted in both angles. Moreover, uncertainties in the derived quantities are readily related to errors in the measured photocurrent and are found to depend on such errors in a manner permitting their accurate determination. Consequently, a method can be implemented which rapidly provides detailed atomic or molecular information, but which also (through measurement of p) can provide an important new technique for calibrating instruments and for measuring optical constants.

1. Introduction

For an ensemble of randomly oriented molecules, the total cross section σ_{tot} for the emission of photoelectrons and the asymmetry parameter β are both important for understanding the geometrical and electronic structure of the molecules comprising the ensemble (Cooper and Zare 1968, 1969, Cooper and Manson 1969, Tully *et al* 1968).

Recently, synchrotron radiation sources have become available for exciting an ensemble of target species by tuning through a continuum of photon energies (Winick and Doniach 1981, Koch *et al* 1983). This possibility of tuning $h\nu$ continuously increases the desirability of finding methods for efficiently collecting electrons (or other photofragments) with detectors which subtend a large solid angle (for good signal-to-noise characteristics at high scan rates of $h\nu$) which is chosen to permit $\sigma_{tot}(h\nu)$ and $\beta(h\nu)$ to be measured as directly as possible. (Here σ_{tot} represents the

total cross section for emission from orbital j, and is often denoted σ_j.) This measurement technique contrasts with historical methods of finding σ_{tot} and β. In these latter cases, scanning of $h\nu$ was not possible, and the use of small solid angle detectors at special angles gave adequate count rates for measurements at the few photon energies available (Samson 1970, Carlson 1975).

We deal in this paper with a specific detector geometry, chosen to give either σ_{tot} alone, or to give jointly σ_{tot}, β and the incident light polarisation p with high efficiency using extended solid angles for the detector acceptance region. We consider the special case of unpolarised or only partially polarised radiation incident on an unpolarised molecular ensemble, with photoelectrons collected by a cylindrical mirror analyser (CMA) (a good review is found in Sevier (1972)) with a large (~1 sr) acceptance area. We show that by properly constructing such a system so that one can choose between several acceptance geometries, $\sigma_{tot}(h\nu)$, $\beta(h\nu)$ and the light polarisation $p(h\nu)$ can be rapidly measured where σ_{tot} and β are also functions of electron binding energy E_B. By constructing a CMA with two movable aperture stops, one may rapidly determine with three scans in $h\nu$ all the angular information for a particular target species and binding energy as well as the incident polarisation. Such a procedure can supply detailed information useful for understanding the electronic structure of large numbers of molecules. Further, the measurement of p as a function of $h\nu$ also provides an important new approach to calibrating instrumentation and for the measurement of optical constants in difficult photon energy regions.

2. Vignetting in θ and ϕ of a cylindrical mirror analyser (CMA) aperture for measurement of $\sigma_{tot}(h\nu)$, $\beta(h\nu)$ and $p(h\nu)$

We consider the case shown in figure 1 in which the angular acceptance aperture of a CMA is vignetted so that the polar angle acceptance range is $\theta_1 \leq \theta \leq \theta_2$ and the azimuthal range between $-\phi_t$ and ϕ_t is unobscured. Further, we assume that photons

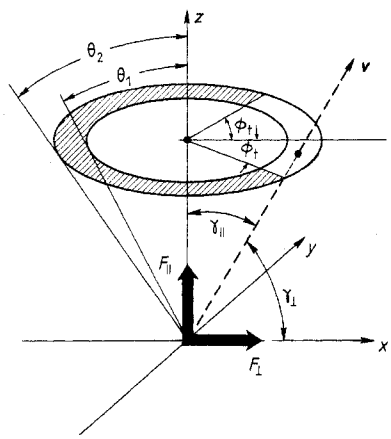

Figure 1. The acceptance aperture of a vignetted CMA is shown, with the velocity vector V of a transmitted electron having polar angles (θ, ϕ) satisfying $\theta_1 \leq \theta \leq \theta_2$; $|\phi| \leq \phi_t$. $F_{||}$ and $F_\perp$ are in the photon polarisation directions, with magnitudes proportional to the two components of photon flux in equation (7).

are incident in the y direction, with fluxes $F_\perp$ and $F_\parallel$ polarised respectively perpendicular to and parallel to the z axis. This case represents, for example, that of a storage ring or other light source incident in the $+y$ direction into an experimental chamber in which a CMA is oriented with its axis in the z direction and its acceptance volume centred on the origin of the coordinate system.

Referring to figure 1, the differential photocurrent $dJ_\perp$ due to the flux $F_\perp$ of photons polarised perpendicular to the z axis is

$$dJ_\perp = F_\perp K \frac{\sigma_{tot}}{4\pi}[1+\beta P_2(\cos\gamma_\perp)]\,d\Omega \tag{1a}$$

where K is a constant, $\gamma_\perp$ is the angle between $F_\perp$ and the detection direction $\hat{V}$, and $P_2(x)=\frac{1}{2}(3x^2-1)$ is the second Legendre polynomial. The corresponding relation for $dJ_\parallel$ is:

$$dJ_\parallel = F_\parallel K \frac{\sigma_{tot}}{4\pi}[1+\beta P_2(\cos\gamma_\parallel)]\,d\Omega. \tag{1b}$$

In the following, we set $K=1$ for convenience. The integral of equation (1b) over the analyser acceptance solid angle Ω_0 gives

$$\frac{4\pi J_\parallel}{\Omega_0} = F_\parallel \sigma_{tot}(1+\beta T) \tag{2}$$

where T depends on the analyser geometry only through the angles θ_1 and θ_2. In equation (2), T is given by

$$T \equiv \left(\int_{\theta_1}^{\theta_2} P_2(\cos\theta)\sin\theta\,d\theta\right)(\cos\theta_1-\cos\theta_2)^{-1}. \tag{3}$$

As will be shown below, the choice of two ranges of the limits of integration in equation (3), for which $T=0$ in one case and $T\neq 0$ in the other, will permit determination of the radiation polarisation p as well as σ_{tot} and β.

We begin our analysis by deriving an expression for the total photocurrent integrated over the detector aperture illustrated in figure 1, and due to both photon polarisations.

We integrate (1a) over Ω_0 using the addition theorem for spherical harmonics:

$$P_2(\cos\gamma_\perp) = \tfrac{4}{5}\pi \sum_{m=-2}^{2} Y_2^{m^*}(\theta,\phi)\,Y_2^m(\theta',\phi').$$

We integrate the electron direction (θ,ϕ) over Ω_0, and set (θ',ϕ'), the polarisation vector direction, equal to $(\pi/2, 0)$. We obtain

$$\frac{4\pi J_\perp}{\Omega_0} = F_\perp \sigma_{tot}\left(1-\frac{\beta T}{2}+\beta(1-T)\frac{\sin 2\phi_t}{4\phi_t}\right). \tag{4}$$

The total measured photocurrent is

$$J_{tot} = J_\parallel + J_\perp. \tag{5}$$

Although in general the source may be elliptically polarised (e.g., in the case of a synchrotron radiation source), one can show quite generally that the parallel and perpendicular components of the electric vector of the light beam cause independent

photocurrents as long as the detector is not oriented (Samson and Starace 1975) (does not distinguish for example between different electron spins) and the target is not chiral.

Using (5), we finally obtain

$$\frac{4\pi J_{\text{tot}}}{\Omega_0} = F\sigma_{\text{tot}}\left\{1+\frac{\beta}{2}\left[\left(\frac{T}{2}+(1-T)f(\phi_t)\right)+p\left(\frac{3T}{2}-(1-T)f(\phi_t)\right)\right]\right\} \quad (6)$$

where F is the total incident flux

$$F \equiv F_{\parallel}+F_{\perp} \quad (7)$$

p is the polarisation

$$p \equiv \frac{F_{\parallel}-F_{\perp}}{F_{\parallel}+F_{\perp}} \quad (8)$$

and

$$f(\phi_t) \equiv \frac{\sin 2\phi_t}{4\phi_t}. \quad (9)$$

The function $f(\phi_t)$ is plotted in figure 2. In deriving equation (6), we use the identities $F_{\parallel}/F = (1+p)/2$ and $F_{\perp}/F = (1-p)/2$. See the review by Krause (1981) and the references therein for a rather complete discussion of the origin and measurement of photoelectron currents from atoms and molecules.

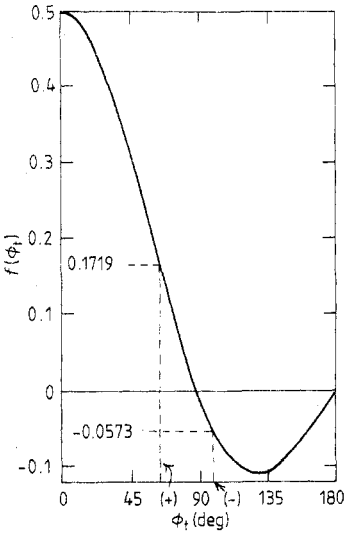

Figure 2. The function $f(\phi_t) = \sin 2\phi_t/4\phi_t$, which is defined in equation (9). We indicate the special values of the function $f(\phi_t)$ (0.1719 and −0.0573) which are used in § 4, and values of ϕ_t which are used to obtain these points on the curve.

3. Solution of the equations for σ_{tot}, β and p

Equation (6) is the basic relation between the measured current J_{tot} and the three unknown quantities σ_{tot}, β and p. Upon initial examination, it might be thought that equation (6) should allow determination of the cross section and asymmetry parameter

(at a given binding energy), and the polarisation at a given photon energy by varying ϕ_t alone and performing three independent measurements. Unfortunately, the structure of equation (6) does not allow such a simple approach for two reasons:

(i) the measured quantity J_{tot} is scaled by σ_{tot}; and

(ii) when equation (6) is written as a 3×3 linear equation, the determinant of the coefficient matrix vanishes. This section examines the mathematical and operational (experimental) procedures which are needed to solve this problem.

A first step is to rearrange the factors in equation (6) and define some terms. We assume that the variation of F with $h\nu$ is measured by using a calibrated photodiode at the sample point (e.g., an Al_2O_3 photocathode or a sample gas for $\sigma_{tot}(h\nu)$ is known). Then we define the normalised measured photocurrent M as

$$M \equiv \frac{4\pi J_{tot}}{F\Omega_0} \tag{10}$$

which represents the measured quantity normalised for the effects of changing incident flux or analyser acceptance solid angle. We will treat M as the fundamental measured quantity.

Now, rearrange equation (6) by multiplying by $1/F\sigma_{tot}$ and moving terms multiplied by β to the left-hand side. This procedure gives:

$$MW_0 - [\tfrac{1}{2}T + (1-T)f]W_1 - [\tfrac{3}{2}T - (1-T)f]W_2 = 1 \tag{6a}$$

where

$$W_0 \equiv 1/\sigma_{tot} \tag{11}$$

$$W_1 \equiv \beta/2 \tag{12}$$

and

$$W_2 \equiv p\beta/2. \tag{13}$$

Our initial strategy is to determine W_0, W_1 and W_2 by forming three separate linear equations from (6*a*), each one representing a measurement at a different value of ϕ_t ($\phi_t = \phi_t^{(0)}$, $\phi_t^{(1)}$ and $\phi_t^{(2)}$). We denote by f_0, f_1 and f_2 the values of $f(\phi_t)$ obtained at these three values of ϕ_t, and by M_0, M_1 and M_2, the corresponding measured values of M for these three analyser geometries. The unknown W_k are then determined by the 3×3 problem

$$\begin{pmatrix} M_0 & -[\frac{1}{2}T + (1-T)f_0] & -[\frac{3}{2}T - (1-T)f_0] \\ M_1 & -[\frac{1}{2}T + (1-T)f_1] & -[\frac{3}{2}T - (1-T)f_1] \\ M_2 & -[\frac{1}{2}T + (1-T)f_2] & -[\frac{3}{2}T - (1-T)f_2] \end{pmatrix} \begin{pmatrix} W_0 \\ W_1 \\ W_2 \end{pmatrix} = \begin{pmatrix} 1 \\ 1 \\ 1 \end{pmatrix} \tag{14}$$

or, more compactly

$$\mathbf{A}\boldsymbol{W} = \boldsymbol{e} \tag{15}$$

where $\mathbf{A}$ is the matrix in equation (14), $\boldsymbol{W}$ is the solution vector of interest, and $\boldsymbol{e}$ is the unit vector.

Equation (15) can be used to show the singular nature of the problem of interest. Furthermore, this equation, along with relations arising from it and from (6*a*), which are discussed in an appendix, provide the means to determine σ_{tot}, β and p to check the validity of data collected during the measurement of photoelectron fluxes.

Summarising the results of the appendix, it is easily shown that Det $\mathbf{A} = 0$ so that a unique solution to (15) does not exist. Further, the result that the determinant of some 2×2 submatrix of $\mathbf{A}$ does not vanish shows that there exists a *particular* solution of (15) with two non-vanishing components:

$$\mathbf{A}\boldsymbol{W}_{\mathrm{p}} = \boldsymbol{e} \tag{16a}$$

where for T non-zero

$$\boldsymbol{W}_{\mathrm{p}} = \begin{pmatrix} 0 \\ -(2T)^{-1} \\ -(2T)^{-1} \end{pmatrix}. \tag{16b}$$

The general solution to equation (15), for T non-zero, is given by adding to $\boldsymbol{W}_{\mathrm{p}}$ a solution $\boldsymbol{W}_{\mathrm{h}}$ of equation (15) in which the right-hand side is zero (the homogeneous solution) multiplied by a free parameter λ:

$$\boldsymbol{W} = \boldsymbol{W}_{\mathrm{p}} + \lambda \boldsymbol{W}_{\mathrm{h}}. \tag{17}$$

In the appendix, it is shown that $\boldsymbol{W}_{\mathrm{h}}$ can be written in the form:

$$\boldsymbol{W}_{\mathrm{h}} = \begin{pmatrix} 2T \\ R + 3TS/2(1-T) \\ R - TS/2(1-T) \end{pmatrix}. \tag{18}$$

S and R are invariants and are given by:

$$S \equiv \frac{M_i - M_j}{f_i - f_j} \qquad \text{and} \qquad R \equiv M_i - f_i S \qquad \text{for } i, j = 0, 1, 2;\ i \neq j. \tag{19}$$

The general solution (for the form of $\boldsymbol{W}_{\mathrm{h}}$ given in (18)) is then

$$\begin{pmatrix} W_0 \\ W_1 \\ W_2 \end{pmatrix} = \begin{pmatrix} 1/\sigma_{\mathrm{tot}} \\ \beta/2 \\ p\beta/2 \end{pmatrix} = \begin{pmatrix} 2\lambda T \\ -(2T)^{-1} + \lambda[R + 3TS/2(1-T)] \\ -(2T)^{-1} + \lambda[R - TS/2(1-T)] \end{pmatrix}. \tag{20}$$

Equation (20) can now be used to develop a strategy for determining σ_{tot}, β and p.

4. Procedure for measuring σ_{tot}, β and p

The presence of λ in (20) shows that three measurements of J_{tot} against ϕ_{t} are not sufficient at binding energy E_{B} to determine σ_{tot} and β as well as p. An independent means of determining λ must first be used, and variation of ϕ_{t} alone does not provide enough information. Consequently, we propose that the CMA also provides a method for varying the polar angle range—a second degree of vignetting adjustment.

Our procedure is first to choose θ_1 and θ_2 so that T vanishes, and to choose ϕ_{t} so that $f(\phi_{\mathrm{t}}) = 0$. (Determination of θ_1 and θ_2 so that $T(\theta_1, \theta_2) = 0$ is discussed in the appendix.) For this geometry, as equation (6) shows, J_{tot} depends only on σ_{tot}.

This independent measurement of σ_{tot} can now be used in (20) for non-vanishing T to fix λ. Thus, the analyser is next changed to a configuration in which T is substantially different from zero so that β and p in the second and third components of equation (20) depend with higher accuracy on the measured quantities M_1 and M_2, which determine S and R (see equation (19)).

Now only two different values of ϕ_t, i.e., two additional scans in $h\nu$, are needed to determine the remaining quantities β and p.

By considering a specific example, it becomes clear how this general result can be implemented experimentally. We propose an explicit set of procedures and analyser geometries which can be used to determine σ_{tot}, β and p. This example also shows the practical significance of our work by giving the precision with which β and p can be determined as a function of the precision of the measurements of the photocurrents obtained for different geometries, and of the precision with which the apparatus can achieve the desired geometries.

We propose vignetting of the analyser to achieve three specific analyser aperture geometries (described in table 1) for which equation (6) takes special, simple forms. These geometries are labelled 0, +, and −, and for each geometry the relevant symbol is used as a superscript on quantities such as acceptance solid angle, or photocurrent, which are achieved at that analyser geometry.

Table 1. Analyser geometries for the example of § 4.

Geometry	θ_1 (deg)	θ_2 (deg)	ϕ_t (deg)	$T(\theta_1, \theta_2)$	$f(\phi_t)$	Ω_0 (sr)
0	46.60	62.60	90	0	0	0.7128
+	46.60	54.60	64.59	0.1028	0.1719	0.2431
−	46.60	54.60	102.05	0.1028	−0.0573	0.3840

Geometry '0' is the one for which $T(\theta_1, \theta_2)$ and $f(\phi_t)$ are both zero. In that case, equation (6) reduces to:

$$\sigma_{tot} = \frac{4\pi J_{tot}^{(0)}}{F\Omega_0^{(0)}}. \tag{21}$$

This special geometry yields a signal directly proportional to σ_{tot}, independent of β and p. It satisfies the requirement that the free parameter λ of the previous section must be determined with an analyser geometry which changes the structure of equation (6).

Next we consider the geometries '+' and '−'. In these geometries, the analyser polar angle acceptance range is changed to one in which $T(\theta_1, \theta_2)$ is substantially non-zero, and is the same for both of these cases. This value of $T(\theta_1, \theta_2)$ is denoted T_m. Then ϕ_t is set at one of two different values, for which $f(\phi_t)$ is equal to

$$\frac{3T_m}{2(1-T_m)} \quad \text{or} \quad -\frac{T_m}{2(1-T_m)}$$

causing in each case one of the terms in large round brackets in equation (6) to vanish. Thus, we obtain for geometry '+'

$$\frac{4\pi J_{tot}^{(+)}}{F\Omega_0^{(+)}} = \sigma_{tot}(1+\beta T_m) \tag{22}$$

and for geometry '−'

$$\frac{4\pi J_{tot}^{(-)}}{F\Omega_0^{(-)}} = \sigma_{tot}(1+\beta p T_m). \tag{23}$$

Next we divide equation (22) by equation (21) and solve for β in terms of the ratio of photocurrents $J_{\text{tot}}^{(0)}$ and $J_{\text{tot}}^{(+)}$:

$$\beta = T_{\text{m}}^{-1}\left(\frac{J_{\text{tot}}^{(+)}}{J_{\text{tot}}^{(0)}}\frac{\Omega_0^{(0)}}{\Omega_0^{(+)}} - 1\right). \tag{24}$$

Similarly, we can divide equation (23) by equation (21) to obtain the polarisation

$$p = (\beta T_{\text{m}})^{-1}\left(\frac{J_{\text{tot}}^{(-)}}{J_{\text{tot}}^{(0)}}\frac{\Omega_0^{(0)}}{\Omega_0^{(-)}} - 1\right). \tag{25}$$

The solutions in equations (24) and (25) exhibit all of the properties discovered while analysing the formalism of § 3. They exhibit the singularlity of the solutions $T(\theta_1, \theta_2) \to 0$. In order for β and p to be determined, the measured photocurrents for geometries '+' and '−' are normalised to that measured in geometry '0', which corresponds to the fixing of the free parameter λ. Also, p cannot be determined until β has been found and is substantially non-zero.

We now replace the quantities in equations (24) and (25) by their numerical values from table 1 and obtain

$$\beta = 9.718\left(2.93\frac{J_{\text{tot}}^{(+)}}{J_{\text{tot}}^{(0)}} - 1\right) \tag{26}$$

and

$$p = \frac{9.718}{\beta}\left(1.86\frac{J_{\text{tot}}^{(-)}}{J_{\text{tot}}^{(0)}} - 1\right). \tag{27}$$

These results for β and p are plotted in figures 3 and 4, respectively. Figure 3 shows that $(J_{\text{tot}}^{(+)}/J_{\text{tot}}^{(0)})$ varies from about 0.31 to 0.41 as β varies over the physically meaningful range −1 to 2. A 33% change in the measured ratio covers the entire range within

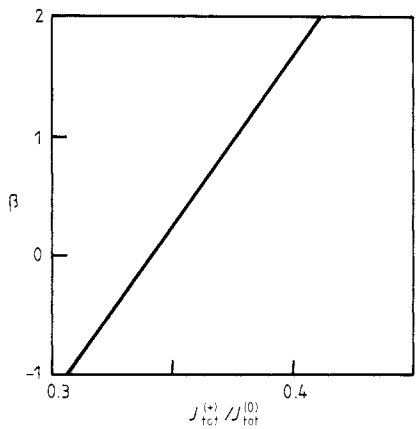

Figure 3. The relationship between $J_{\text{tot}}^{(+)}/J_{\text{tot}}^{(0)}$ and β, from § 4, for the physically accessible values of β.

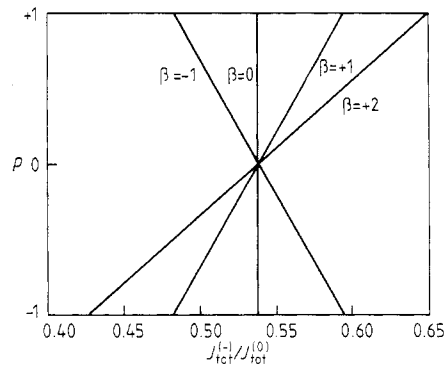

Figure 4. The relationship between $J_{\text{tot}}^{(-)}/J_{\text{tot}}^{(0)}$ and p, from § 4, for the physically meaningful range $-1 \leqslant p \leqslant +1$, for values of β from −1 to +2.

which β is to be found. Consequently, a 1% precision in the measured photocurrent ratio corresponds to a precision in β of about 0.1. Furthermore, in such a set of measurements obtained while scanning $h\nu$, the extrema of $\beta(h\nu)$ would be found to high precision even in the case in which errors in setting the analyser geometry cause the absolute value of β to be somewhat uncertain.

The result for p represented by equation (27) is plotted in figure 4 for different values of β. The most favourable case is for $\beta = 2$. The polarisation then varies over its accessible range $-1 \leqslant p \leqslant +1$ as $J_{\text{tot}}^{(-)}/J_{\text{tot}}^{(0)}$ varies from about 0.43 to 0.65, e.g., by about 50%. In this case a 1% precision in the measured photocurrent ratio represents a precision of about 0.04 in p.

An important application of the technique described here would be the determination of the polarisation of synchrotron radiation in a sample region, as a function of photon energy. For this purpose, a simple closed-shell atomic vapour with s-electron emission (e.g., He gas) would represent an ideal calibration sample, since for such a gas the emission well above threshold would give $\beta = 2$. Once $p(h\nu)$ was determined from equation (27) in this manner, the determination of β for an arbitrary species could proceed using equation (6) directly, i.e., by making two measurements (at different values of ϕ_t) leaving the polar angular acceptance range fixed. This technique could also be used to help determine optical constants of a reflecting sample by measuring its effect on $p(h\nu)$.

When using synchrotron radiation, the value of $p(h\nu)$ is fixed and it is very awkward to change the spatial orientation of the corresponding polarisation ellipse. However, this is not the case for most laboratory light sources, such as lasers. For such sources, it is usually straightforward to rotate the polarisation ellipse. It is useful to consider what CMA detection strategy could then be employed. Call $J_{\text{tot}}^{(1)}$ the total photocurrent obtained with a flux $F_{\parallel}$ along z and $F_{\perp}$ along x; call $J_{\text{tot}}^{(2)}$ the total photocurrent with $F_{\parallel}$ along x and $F_{\perp}$ along z. Then it follows from equation (6) that:

$$\frac{4\pi(J_{\text{tot}}^{(1)} + J_{\text{tot}}^{(2)})}{\Omega_0} = 2F\sigma_{\text{tot}}\left[1 + \frac{\beta}{2}\left(\frac{T}{2} + (1-T)f(\phi_t)\right)\right]. \tag{28}$$

Hence the sum of $J_{\text{tot}}^{(1)}$ and $J_{\text{tot}}^{(2)}$ is independent of p. Moreover, once again σ_{tot} and β can be found simply by appropriately vignetting (in ϕ_t) the CMA while leaving the polar angular acceptance range fixed. Finally, this last result (equation (28)) can be used with synchrotron sources provided one is able to rotate the CMA about the y axis.

5. Summary and conclusions

In the analysis in this paper, we have discovered several interesting facts concerning the determination of all three quantities σ_{tot}, β and p by vignetting a CMA. We have seen that the mathematical structure of the fundamental equation (6) is such that two separate angular vignetting degrees of freedom must be used in order to determine these three quantities unambiguously.

Variation of ϕ_t alone always results in solutions with a free, undetermined parameter. One must first set $T = 0$ by proper choice of θ_1 and θ_2 in order to determine σ_{tot}. Then θ_1 and θ_2 are changed so that T is substantially different from 0 in order to find β and p. While the first step proceeds with an analyser whose polar angular acceptance range includes the 'magic angle' (Samson 1969, Samson and Gardner

Table 2. Location of the detector centre, x, as a function of the acceptance half-angle ε so that $T = 0$. This gives the polar angle acceptance range $\theta_1 \leq \theta \leq \theta_2$.

ε (deg)	x (deg)	θ_1 (deg)	θ_2 (deg)
0	54.74	54.74	54.74
5	54.68	49.68	59.68
10	54.52	44.52	64.52
15	54.24	39.52	69.52
20	53.80	33.80	73.80
25	53.17	28.17	78.17
30	52.24	22.24	82.24
35	50.86	15.86	85.86
40	48.70	8.70	88.70
45	45.00	0.00	90.00

1972) θ_M ($\theta_M \equiv \cos^{-1} 3^{-1/2}$)), it can provide large flux due to the significant range in θ which can be chosen (table 2), which permits relatively fast scans in $h\nu$ and the measurement of σ_{tot} for a large number of binding energies in a short time. This is in contrast to early detectors based on use of the magic angle for σ_{tot} measurements—detectors in which the solid angle of acceptance was small.

The theory also provides a means for correcting for systematic errors due to non-ideal detector construction which might render the analyser acceptance not precisely proportional to ϕ_t. For example, measurements of J_{tot} for several values of ϕ_t can be used with equation (19) to check the internal consistency of the measurements due to the fact that the ratio S or the quantity R in equation (19) is an invariant which is independent of ϕ_t.

Measurements of p in the vacuum ultraviolet and soft x-ray regions can be difficult, especially at large photon energies for which reflection-based techniques are inefficient. The present method constitutes a new approach to such measurements, using an appropriately chosen sample gas and a modified CMA. The theory we have described requires, however, that an orbital with β significantly different from 0 be chosen in a given range of photon energy if p is to be determined. Determination of p in relation to $h\nu$ can prove valuable for experiments in which the degree of polarisation is unknown due to uncertain optical constants for gratings and other optical elements in VUV and soft x-ray monochromators.

Also, $p(h\nu)$ can be measured after reflection from specular samples at several different angles of incidence to provide a new and potentially powerful technique for the determination of optical constants in experimentally difficult ranges of photon energy.

Finally, note that implementation of the technique suggested here requires significant modification of the usual CMA design. The variable apertures used for vignetting must be implemented in a way which does not affect the detected photocurrent except through the solid-angle effect. A good way to achieve this goal is through use of variable apertures near the electron detector rather than near the sample region. Near the detector, electron optics can be used to accelerate the electrons prior to vignetting so that varying contact potentials in the vignetting aperture mechanism are unimportant. The technique can in this case work with minimal systematic errors even with pass energies of only a few eV, for which the apertures suggested in table 1 give resolution sufficient to resolve vibrational structure.

Acknowledgment

We wish to thank C Denise Caldwell who corrected a significant error in the derivation leading to equation (6) in an earlier version of this paper. One of us (RNZ) gratefully acknowledges support of the National Science Foundation under NSF PHY 82-06400.

Appendix

In this mathematical appendix, we cover two topics. We first derive the relationship between θ_1 and θ_2 which ensures that $T(\theta_1, \theta_2) = 0$ (see equation (3)), thereby describing the polar angle range used for determination of σ_{tot} independently of β and p. Then a discussion of the structure of equation (14) and of its solutions follows, for the general case in which T is non-zero.

A.1. Values of θ_1 and θ_2 for which $T(\theta_1, \theta_2) = 0$

We define angles x and ε such that

$$\theta_1 = x - \varepsilon \qquad \theta_2 = x + \varepsilon. \tag{A.1}$$

For $\cos\theta_1 \neq \cos\theta_2$, we find by substituting equation (A.1) into equation (3) and setting T equal to zero:

$$\cos^2(x+\varepsilon) + \cos(x+\varepsilon)\cos(x-\varepsilon) + \cos^2(x-\varepsilon) = 1. \tag{A.2}$$

With the use of the identities $\cos(x+\varepsilon) = \cos x \cos\varepsilon - \sin x \sin\varepsilon$ and $\cos(x-\varepsilon) = \cos x \cos\varepsilon + \sin x \sin\varepsilon$, equation (A.2) reduces to the expression

$$\cos^2 x = \frac{\cos^2\varepsilon}{4\cos^2\varepsilon - 1} \tag{A.3}$$

which has the solution

$$x = \cos^{-1}\left(\frac{\cos^2\varepsilon}{4\cos^2\varepsilon - 1}\right)^{1/2}. \tag{A.4}$$

Equation (A.4) expresses the detector location x as a function of the detector half-angle ε. Table 2 lists some typical solutions of equation (A.4). We conclude that for large finite acceptance angles, the detector should be placed at a polar angle close to the magic angle. Indeed, the position of the detector is surprisingly insensitive to the value of the half-angle for values of $\varepsilon < 20°$, differing from the magic angle by less than one degree.

Alternatively we may use equation (A.3) to express the detector half-angle as a function of the detector location. We find

$$\varepsilon = \cos^{-1}\left(\frac{\cos^2 x}{4\cos^2 x - 1}\right)^{1/2} \tag{A.5}$$

which has the same functional dependence as equation (A.4). Equations (A.4) and (A.5) show that x and ε satisfy the identity

$$(4\cos^2 x - 1)(4\cos^2\varepsilon - 1) = 1. \tag{A.6}$$

The maximum value of ε is 45° corresponding to the detection of all flux in one hemisphere.

A.2. The solution of equation (14)

If system (14), with T chosen non-zero, has a solution for a finite value of σ_{tot}, then there exists a one-parameter family of solutions. The determination of these solutions is here discussed for the general case of non-zero T, which is the form of the problem which must be addressed in order to find the three unknown quantities of interest. In § 4 we also consider the special case $T = 0$, which fixes the physically correct value of the free parameter which is left undetermined in the general case for which T is non-zero.

To find the general (non-zero T) solution, we first introduce the following cyclic difference vector

$$(\Delta f)^T = (f_1 - f_2, f_2 - f_0, f_0 - f_1). \tag{A.7}$$

This vector is perpendicular to the right-hand side, $\boldsymbol{e}$, of (14) and to the second and third columns of the coefficient matrix $\mathbf{A}$. Thus

$$0 = (\Delta f)^T \boldsymbol{e} = (\Delta f)^T (\mathbf{A}\boldsymbol{W}) = [(\Delta f)^T \boldsymbol{M}](1/\sigma_{\text{tot}}).$$

Since σ_{tot} is finite, we have

$$(\Delta f)^T \boldsymbol{M} = 0. \tag{A.8}$$

Expanding the determinant of $\mathbf{A} = \det(\mathbf{A})$ along the first column yields

$$\det(\mathbf{A}) = 2T(1-T)(\boldsymbol{M}^T \Delta f) = 0. \tag{A.9}$$

Since $2T(1-T)(f_i - f_j) \neq 0$ in general for $i \neq j, i, j = 0, 1, 2$, the matrix $\mathbf{A}$ has rank 2 (i.e., there is at least one 2×2 submatrix of $\mathbf{A}$ with non-zero determinant). There is a theorem (see for example Hohn 1958) which states that in such a case, when the left null vector $\boldsymbol{g}$ of $\mathbf{A}$ ($\boldsymbol{g}^T \mathbf{A} = 0$) also satisfies $\boldsymbol{g}^T \boldsymbol{e} = 0$ then there exists a one-parameter family of solutions of equation (14) of the form

$$\boldsymbol{W} = \boldsymbol{W}_{\text{p}} + \lambda \boldsymbol{W}_{\text{h}} \tag{A.10}$$

where λ is a free parameter, $\boldsymbol{W}_{\text{p}}$ is a particular solution ($\boldsymbol{A}\boldsymbol{W}_{\text{p}} = \boldsymbol{e}$), and $\boldsymbol{W}_{\text{h}}$ is a solution to the system, $\boldsymbol{A}\boldsymbol{W}_{\text{h}} = 0$. In this case, $\boldsymbol{g} = \Delta f$ satisfies these conditions.

To obtain $\boldsymbol{W}_{\text{p}}$ we set $\boldsymbol{W}_0 = 0$ and then $\boldsymbol{W}_1 = \boldsymbol{W}_2 = -(2T)^{-1}$.

In order to determine $\boldsymbol{W}_{\text{h}}$ we note that if we substract equation (6*a*) for M_j from equation (6*a*) for M_i with $i \neq j$, then

$$(M_i - M_j) W_0 - (1-T)(f_i - f_j)(W_1 - W_2) = 0$$

so

$$\frac{M_i - M_j}{f_i - f_j} = \frac{W_1 - W_2}{W_0}(1-T)$$

is an invariant, i.e., does not depend on which pair (i, j) we choose.

We define the invariants

$$S \equiv \frac{M_i - M_j}{f_i - f_j} \qquad i \neq j, i, j = 0, 1, 2 \tag{A.11}$$

and

$$R \equiv M_i - f_i S. \tag{A.12}$$

R can be seen to be independent of i by forming the difference $(M_i - f_i S) - (M_j - f_j S)$ which vanishes for any i, j.

In the homogeneous case the 0, 1 and 2 components of $\boldsymbol{W}_h$ are in the same proportion as the cofactors of the components of the first row of $\mathbf{A}$ since $\det(\mathbf{A}) = 0$. That is, the first, second and thrid components of the homogeneous solution are equal respectively to the following three determinants (which may be all multiplied by an arbitrary constant):

$$\begin{vmatrix} -[\frac{1}{2}T + (1-T)f_1] & -[\frac{3}{2}T - (1-T)f_1] \\ -[\frac{1}{2}T + (1-T)f_2] & -[\frac{3}{2}T - (1-T)f_2] \end{vmatrix} = 2T(1-T)(f_1 - f_2)$$

$$\begin{vmatrix} -[\frac{3}{2}T - (1-T)f_1] & M_1 \\ -[\frac{3}{2}T - (1-T)f_2] & M_2 \end{vmatrix} = [R(1-T) + \tfrac{3}{2}TS](f_1 - f_2)$$

$$\begin{vmatrix} M_1 & -[\frac{1}{2}T + (1-T)f_1] \\ M_2 & -[\frac{1}{2}T + (1-T)f_2] \end{vmatrix} = [R(1-T) - \tfrac{1}{2}TS](f_1 - f_2).$$

Thus, within a multiplicative constant, the homogeneous solution is

$$\boldsymbol{W}_h = \begin{pmatrix} 2T \\ R + 3TS/2(1-T) \\ R - TS/2(1-T) \end{pmatrix}. \tag{A.13}$$

This result for the homogeneous solution is derived by using the properties of the matrix which is adjoint to $\mathbf{A}$ (see the discussion of the adjoint matrix in Hohn 1958). If $\mathbf{B}$ is adjoint to $\mathbf{A}$ then

$$\mathbf{AB} = \mathbf{BA} = \det(\mathbf{A})\mathbf{I}$$

where $\mathbf{I}$ is the unit matrix. Since $\det(\mathbf{A}) = 0$, the columns of $\mathbf{B}$ are solution vectors to the homogeneous equation, and are all the same within a multiplicative constant. However, from Hohn (1958) the components of a column of $\mathbf{B}$ are the cofactors of the rows of $\mathbf{A}$. (That is, the adjoint matrix $\mathbf{B}$ is the transpose of the matrix of cofactors of $\mathbf{A}$.) This property then leads to the construction of the homogeneous solution from the cofactors of a row of $\mathbf{A}$ as was done above.

References

Carlson T A 1975 *Photoelectron and Auger Spectroscopy* (New York: Plenum)

Cooper J and Zare R N 1968 *J. Chem. Phys.* **48** 942

—— 1969 *Lectures in Theoretical Physics* vol II (New York: Gordon and Breach)

Cooper J W and Manson S T 1969 *Phys. Rev.* **177** 157

Hohn F E 1958 *Elementary Matrix Algebra* (New York: MacMillan) pp 135–8

Koch E E, Eastman D E and Farge Y (ed) 1983 *Handbook on Synchrotron Radiation* vol I (Amsterdam: North-Holland)

Krause M O 1981 *Synchrotron Radiation Research* ed H Winick and S Doniach (New York: Plenum) pp 101–57

Samson J A R 1969 *J. Opt. Soc. Am.* **59** 356

—— 1970 *Phil. Trans. R. Soc.* A **268** 141

Samson J A R and Gardner J L 1972 *J. Opt. Soc. Am.* **62** 856
Samson J A R and Starace A F 1975 *J. Phys. B: At. Mol. Phys.* **8**
Sevier K D 1972 *Low Energy Electron Spectrometry* (New York: Wiley-Interscience)
Tully J C, Berry R S and Dalton B J 1968 *Phys. Rev.* **176** 95
Winick J C and Doniach S (ed) 1981 *Synchrotron Radiation Research* (New York: Plenum)